Accepted Manuscript

Design, synthesis and biological evaluation of [1,2,4]triazolo[1,5-a]pyrimidines as potent lysine specific demethylase 1 (LSD1/KDM1A) inhibitors

Shuai Wang, Li-Jie Zhao, Yi-Chao Zheng, Dan-Dan Shen, Er-Fei Miao, Xue-Peng Qiao, Li-Juan Zhao, Ying Liu, Ruilei Huang, Bin Yu, Hong-Min Liu

PII: S0223-5234(16)30883-2

DOI: 10.1016/j.ejmech.2016.10.021

Reference: EJMECH 8986

To appear in: *European Journal of Medicinal Chemistry*

Received Date: 8 August 2016

Revised Date: 8 October 2016

Accepted Date: 12 October 2016

Please cite this article as: S. Wang, L.-J. Zhao, Y.-C. Zheng, D.-D. Shen, E.-F. Miao, X.-P. Qiao, L.-J. Zhao, Y. Liu, R. Huang, B. Yu, H.-M. Liu, Design, synthesis and biological evaluation of [1,2,4]triazolo[1,5-a]pyrimidines as potent lysine specific demethylase 1 (LSD1/KDM1A) inhibitors, *European Journal of Medicinal Chemistry* (2016), doi: 10.1016/j.ejmech.2016.10.021.

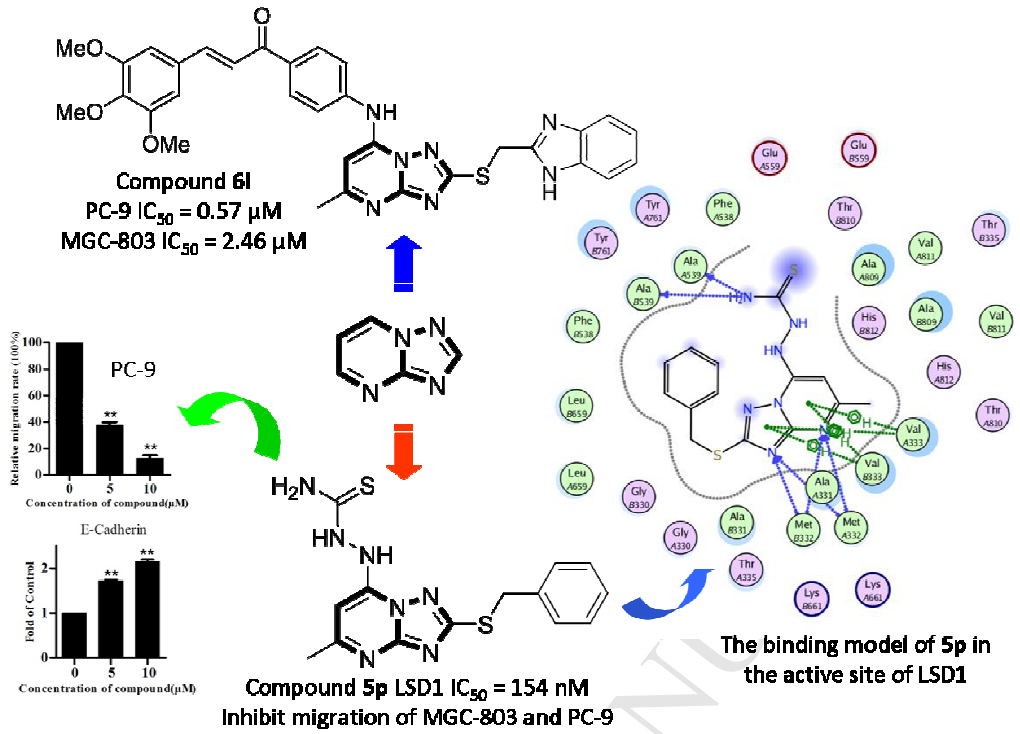

A new series of [1,2,4]triazolo[1,5-a]pyrimidine-based analogs were designed and synthesized. Among them, compound **5p** inactivated LSD1 potently (IC_{50} = 154 nM) and inhibited migration of MGC-803 and PC-9 cells. Compound **6l** showed excellent growth inhibition toward MGC-803 and PC-9 cells.

Design, synthesis and biological evaluation of [1,2,4]triazolo[1,5-a]pyrimidines as potent lysine specific demethylase 1 (LSD1/KDM1A) inhibitors

Shuai Wang[1, #], Li-Jie Zhao[1, #], Yi-Chao Zheng[1], Dan-Dan Shen[1], Er-Fei Miao[1], Xue-Peng Qiao[1], Li-Juan Zhao[1], Ying Liu[1], Ruilei Huang[2], Bin Yu[1, *], Hong-Min Liu[1, *]

[1]School of Pharmaceutical Sciences & Collaborative Innovation Center of New Drug Research and Safety Evaluation, Zhengzhou University, Zhengzhou 450001, China

[2]School of Pharmaceutical Sciences, Central South University, Changsha 410000, China

Abstract: A new series of [1,2,4]triazolo[1,5-a]pyrimidine-based LSD1 inhibitors were designed, synthesized, and further evaluated for their cytotoxicity against MGC-803, EC109, A549 and PC-9 cells as well as the ability of inhibiting LSD1. Some of these compounds showed potent inhibition toward LSD1 and selectively inhibited growth of A549 and PC-9 cells. Compound **6l** potently inhibited growth of PC-9 cells (IC_{50} = 0.59 μM), about 4-fold more potent than 5-FU. Further SARs studies led to the identification of compounds **6l-m**, which had good growth inhibition against all the tested cancer cell lines and were much more potent than 5-FU and **GSK2879552**. Besides, compounds **5p**, **5q** and **6i** inhibited LSD1 potently (IC_{50} = 0.154, 1.19 and 0.557 μM, respectively). Docking studies revealed that compound **5p** formed arene-H interactions with Val333 and hydrogen bonds with surrounding Ala331, Met332, and Ala539 residues. Compound **5p** significantly inhibited migration of A549 and PC-9 cells in a concentration-dependent manner, but had different effect on the expression of E-cadherin and N-cadherin. The [1,2,4]triazolo[1,5-a]pyrimidine scaffold may serve as a starting point for developing potent LSD1 inhibitors for cancer therapy.

Keywords: [1,2,4]triazolo[1,5-a]pyrimidine; Cytotoxicity; LSD1 inactivation; Migration inhibition; Docking studies

1. Introduction

[*]Correspondence and requests for materials should be addressed to *Prof.* Hong-Min Liu (liuhm@zzu.edu.cn) and Dr. Bin Yu (zzuyubin@hotmail.com).

[#]Shuai Wang and Li-Jie Zhao contributed equally to this work.

Lysine specific demethylase 1 (LSD1, also known as KDM1A), the first identified histone lysine specific demethylase in 2004 [1], is a highly conserved flavin adenine dinucleotide (FAD) dependent amino oxidase [2]. In recent years, the biological roles of LSD1 have been partially characterized, such as demethylating p53 [3], or serving as DNA methyltransferase [4] and E2F transcription factor 1 [5], etc, making LSD1 a validated therapeutic target [6]. Additionally, LSD1 was found to be essential for the MLL-rearranged leukemia [7,8]. LSD1 overexpression has been observed in many tumors (e.g. prostate, breast, and gastric cancers, etc) [9], down regulation of LSD1 by siRNA or small molecules has proven to be effective in inhibiting growth of several tumors [10-14]. Therefore, the development of potent LSD1 inhibitors for cancer therapy is highly desirable. To date, a large number of small molecule and peptide-based LSD1 inhibitors have been identified (Fig. 1) [15,16]. 2-PCPA, phenelzine, and pargyline (Fig. 1), initially identified as MAO inhibitors, have been found to be able to inhibit LSD1 weakly [17]. 2-PCPA-based structural modifications have led to the generation of many potent irreversible LSD1 inhibitors [18-20], two of which (ORY-1001 and GSK2879552, Fig.1) have advanced into clinical trials for the treatment of cancers [21,22]. Besides, a large number of reversible LSD1 inactivators have also been identified by us [23-26] and other groups [27]. Following our previous success in the identification of LSD1 inhibitors [23-26], herein we report the design, synthesis and SARs studies of a new series of [1,2,4]triazolo[1,5-a]pyrimidine-based LSD1 inhibitors. Molecular modeling studies were performed to rationalize the potency of newly reported LSD1 inhibitors. The difference of the compounds in inhibiting migration of MGC-803 and PC-9 cells was also investigated.

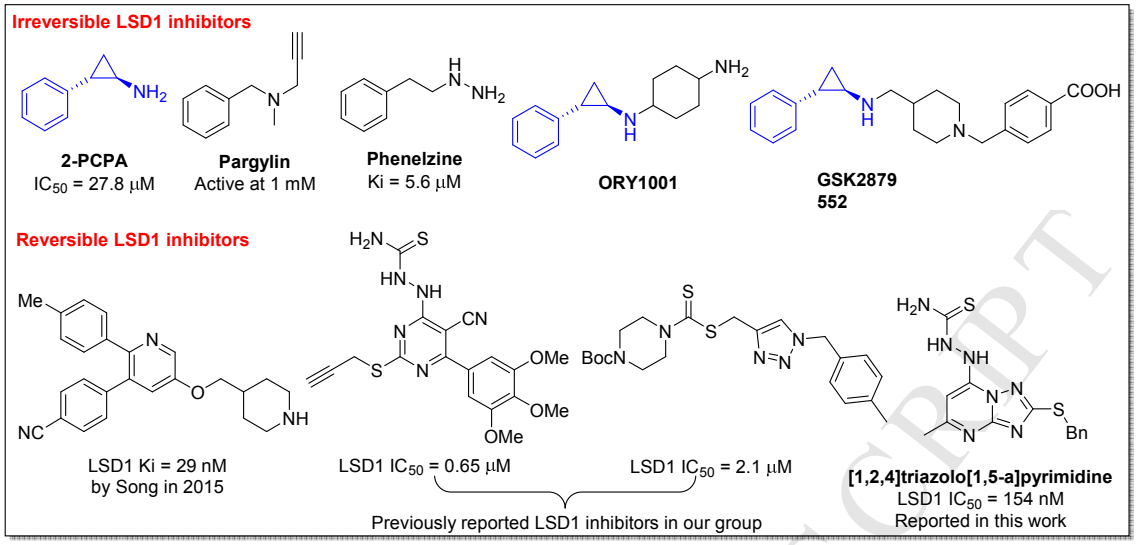

Fig. 1 Some of previously reported LSD1 inhibitors and new inhibitor reported in this work

2. Results and discussion

2.1. Chemistry

The synthesis of compounds **4a-b** is shown in Scheme 1. Treatment of 3-amino-5-mercapto-1,2,4-triazole (**1**) with benzyl chloride or 2-(chloromethyl)benzimidazole in the presence of Na_2CO_3 in acetone gave compounds **2a-b**, which then reacted with ethyl acetoacetate in acetic acid under reflux, affording compounds **3a-b**. Chlorination of compounds **3a-b** using $POCl_3$ as the solvent and chlorinating agent generated the corresponding products **4a-b**.

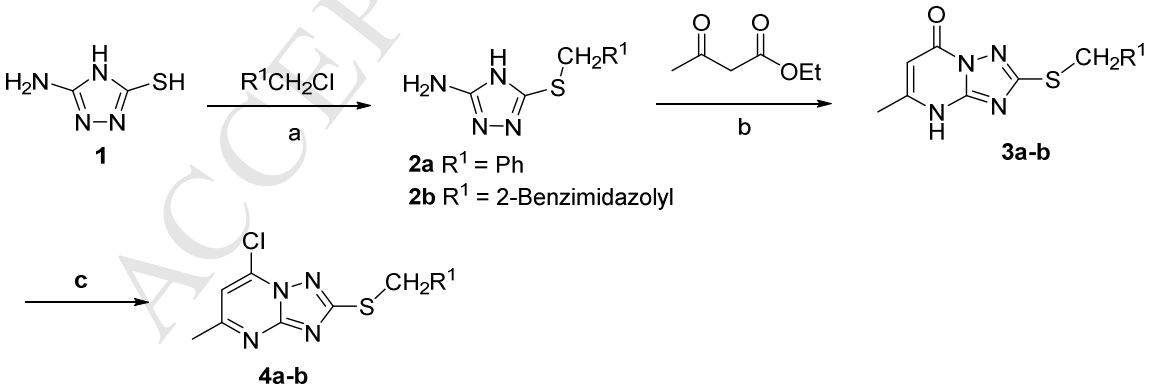

Scheme 1 Synthesis of compounds **4a-b**. Reagents and conditions: (a) Na_2CO_3, acetone, 60 °C, 3-5 h; (b) Acetic acid, 2-15 h, reflux; (c) $POCl_3$, 90 °C, 1 h.

With compounds **4a-b** in hand, we next introduced different amine substituents (alkyl

amines, cycloamines, and anilines) to the [1,2,4]triazolo[1,5-a]pyrimidine scaffold, aiming to achieve substituent diversity and explore the structure-activity relationships (SARs). The detailed synthetic routes of compounds **5a-q** and **6a-m** are given in Schemes 2 and 3. The reactions between different amines and compound **4a** proceeded smoothly and efficiently under mild conditions, giving corresponding products in good yields. Besides, 2-(pyrrolidin-1-yl)ethan-1-ol was also incorporated into this scaffold using a slightly modified protocol (*t*-BuOK, THF, rt), generating an ether-linked analog (**5l**) in 69% yield.

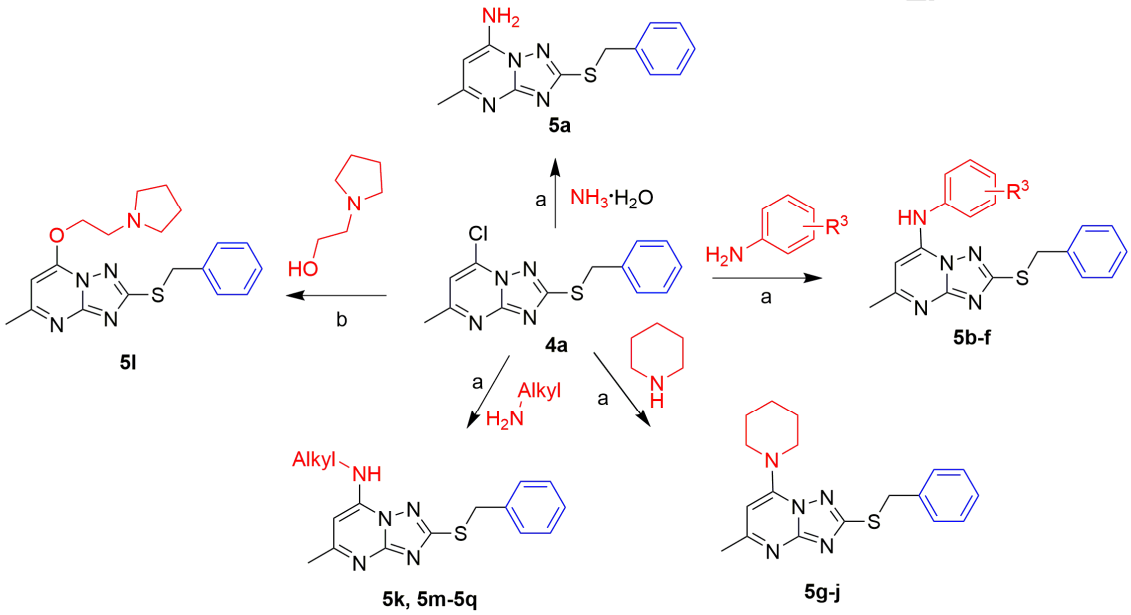

Scheme 2 Synthesis of compounds **5a-q** bearing a benzyl group. Reagents and conditions: (a) EtOH, rt; (b) *t*-BuOK, THF, rt, 10 h.

In order to further investigate the SARs, we also performed additional structural modifications around compound **4b** by introducing different amine substituents. In this design, we introduced the well-known chalcone moiety to the bicyclic *N*-heterocycle core with the purpose of exploring the anticancer activity of such hybrids. More recently, lenalidomide, aminoglutethimide and their structural analogs have drawn increasing attention due to the anticancer efficacy, especially their biological roles as protein degraders for cancer therapy [28-31]. Inspired by these findings, we combined lenalidomide and aminoglutethimide with [1,2,4]triazolo[1,5-a]pyrimidine scaffold [32,33], forming structurally

novel compounds **6k** and **6l**, respectively. All the reactions depicted in Scheme 3 proceeded smoothly in EtOH at room temperature, giving the compounds **6a-m** in good yields.

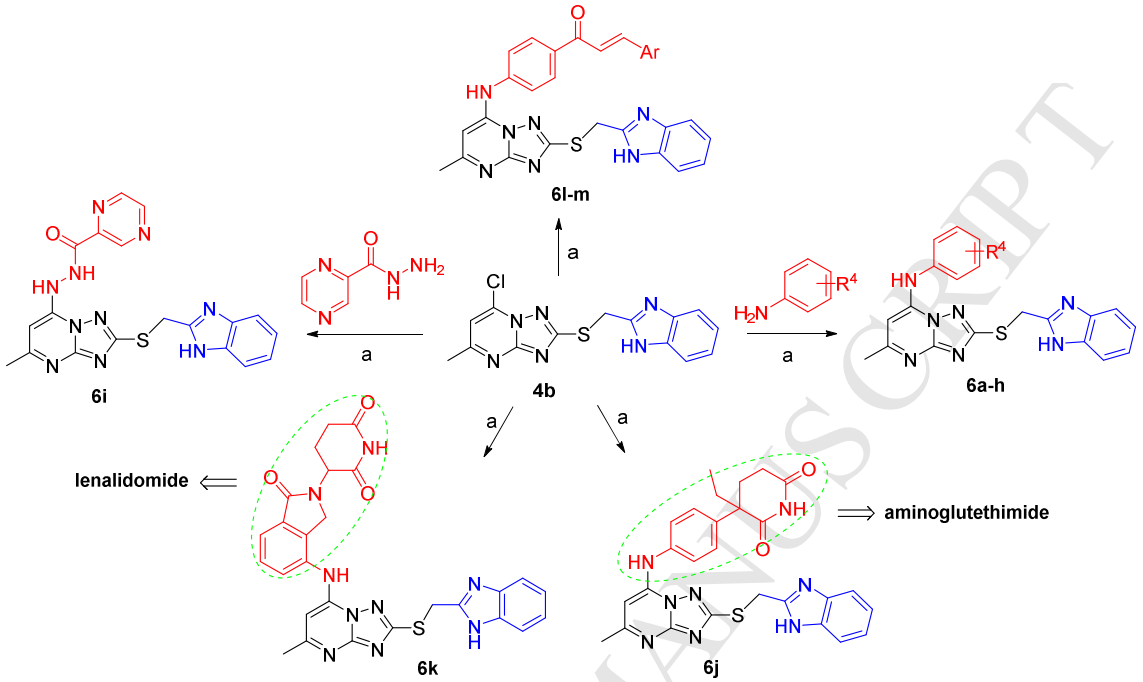

Scheme 3 Synthesis of compounds **6a-m**. Reagents and conditions: (a) EtOH, rt.

2.2. Cytotoxicity evaluation

With these compounds in hand, we next tested their inhibitory activity against four cancer cell lines of different origins (MGC-803, EC109, A549 and PC-9) using the MTT assay. The well-known anticancer drug 5-fluorouracil (5-FU) and **GSK2879552** were used as the control drugs to compare the anticancer efficacy of the synthesized compounds. Initially, the inhibitory effect of compounds **5a-q** and **6a-m** against the tested cancer cell lines was evaluated at 10 μM. The preliminary results are given in Table 1. Generally, compounds **5a-q** were more sensitive to lung cancer cells (A549 and PC-9) and gastric cancer cell MGC-803, regardless of their substituents attached. For EC109 cells, only compounds **5c-e** had around 40% inhibition rate, other compounds with aliphatic amine substituents were less active. However, the inhibitory rate of compound **5f** bearing a terminal carboxylic acid group was 14.3%, significantly lower than those of compounds **5c-e**, which was possibly attributed to the poor cell permeability of compound **5f**. In contrast, compounds **6a-m** selectively inhibited EC109, A549 and PC-9 cells, but were less sensitive to MGC-803 cells (except for

compound **6e**). It is worth noting that compound **6l** bearing the chalcone scaffold showed significantly improved inhibition toward all the tested cancer cell lines, 93.1% inhibition rate was observed for PC-9 cells. However, the structurally similar compound **6m** had a relatively decreased inhibitory rate, indicating the importance of substituents attached to the chalcone scaffold for the activity.

Table 1 Preliminary cytotoxicity of compounds **5a-q** and **6a-m** against several cancer cell lines

Compound	R^1	R^2	Inhibition rate at 10 μM (%)			
			MGC-803	EC109	A549	PC-9
5a	Ph	$-NH_2$	32.3	4.7	57.3	48.3
5b	Ph	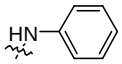	35.0	12.9	50.2	40.2
5c	Ph	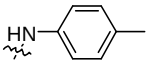	26.0	44.7	33.7	30.2
5d	Ph	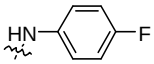	19.7	37.6	41.8	43.5
5e	Ph	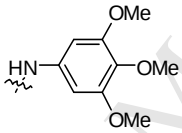	32.8	41.6	37.9	13.5
5f	Ph	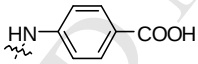	26.7	14.3	34.6	30.7
5g	Ph	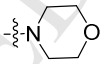	31.0	10.6	45.4	27.3
5h	Ph		32.4	23.9	41.4	29.3
5i	Ph	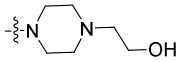	23.8	5.9	42.1	14.9
5j	Ph	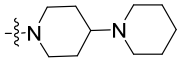	32.8	0.3	56.5	35.6
5k	Ph	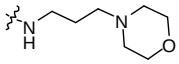	24.9	9.3	49.2	51.9
5l	Ph	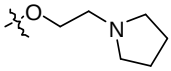	28.8	11.4	49.8	43.6
5m	Ph	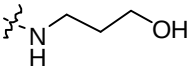	33.3	6.3	53.7	51.4
5n	Ph	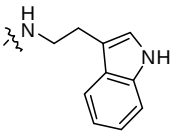	34.2	7.0	43.9	24.0
5o	Ph	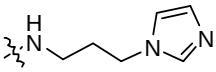	26.2	12.8	50.2	47.7

5p	Ph	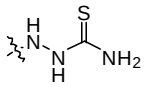	2.1	14.2	25.6	30.7
5q	Ph	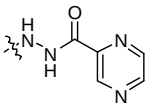	35.3	23.3	40.9	63.2
6a	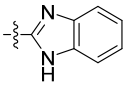	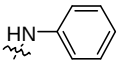	17.9	39.9	38.0	31.6
6b	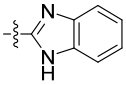	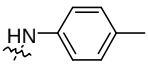	22.9	43.1	35.1	36.9
6c	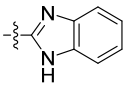	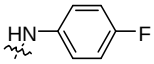	19.2	39.7	36.6	27.6
6d	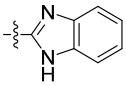	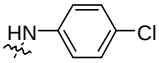	16.8	41.2	34.9	33.2
6e	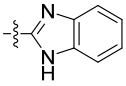	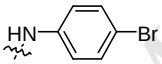	36.7	43.8	35.2	36.4
6f	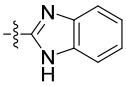	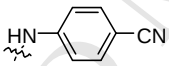	19.3	26.3	52.3	41.9
6g	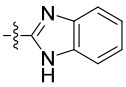	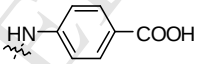	0.4	4.5	5.6	11.9
6h	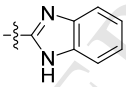	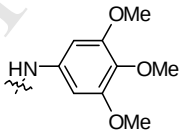	28.0	34.1	52.4	42.9
6i	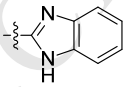	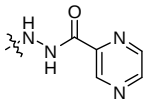	8.6	35.5	65.2	52.5
6j	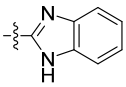	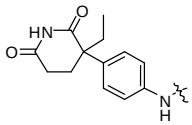	1.1	38.2	49.2	47.9
6k	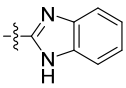	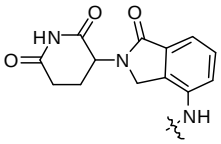	11.4	32.2	48.2	52.4

6l	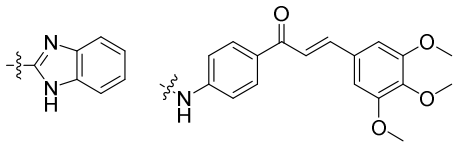		81.3	76.4	71.6	**93.1**
6m	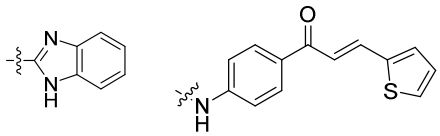		29.6	38.3	51.1	40.4

Based on the above data as shown in Table 1, several compounds with relatively high inhibitory rate were then further evaluated. The IC_{50} values are given in Table 2. Clearly, most of the selected compounds inhibited growth of A549 and PC-9 cells potently with the IC_{50} values ranging from 0.57 to 22.76 μM. For A549 cells, compounds **5a**, **5j**, **5m**, **6i**, **6l** and **6m** were more potent than 5-FU (IC_{50} = 13.95 μM). Compound **6l** showed excellent inhibition toward PC-9 cells with an IC_{50} of 0.57 μM, about 4-fold more potent than 5-FU. Different from other compounds, compounds **6l-m** had good inhibition against the tested cancer cells (IC_{50} < 11 μM) and were more potent than 5-FU and **GSK2879552** (IC_{50} > 50 μM), showing the promising anticancer efficacy of this kind of compounds. From this preliminary studies, we found that molecules combining the chalcone and [1,2,4]triazolo[1,5-a]pyrimidine scaffolds possessed good to excellent cytotoxicity against the tested cancer cells. Compound **6l** may serve as a lead compound for developing more potent anticancer agents targeting PC-9 cells.

Table 2 IC_{50} values of selected compounds against the tested cancer cell lines

Compound	IC_{50} (μM)			
	MGC-803	EC109	A549	PC-9
5a	ND [a]	ND	9.74±0.99	8.14±0.91
5b	ND	ND	16.41±1.22	ND
5j	ND	ND	8.87±0.95	ND
5k	ND	ND	17.03±1.23	15.02±1.12
5l	ND	ND	22.76±1.36	ND
5m	ND	ND	8.85±0.95	10.73±1.03
5o	ND	ND	16.10±1.21	12.26±1.09
5q	ND	ND	ND	12.72±1.10
6f	ND	ND	13.88±1.14	ND
6h	ND	ND	17.96±1.25	ND
6i	ND	ND	10.34±1.02	12.27±1.09
6j	ND	ND	17.50±1.24	12.22±1.09
6k	ND	ND	19.77±1.30	15.01±1.18

6l	2.46±0.39	3.23±0.51	8.79±0.94	0.57±0.24
6m	7.88±0.90	10.58±1.03	9.90±1.00	11.01±1.04
5-FU	10.14±1.00	25.99±1.42	13.95±1.15	1.99±0.30
GSK2879552	>50	>50	ND	ND

[a] ND means no determined

2.3. Prediction of molecular properties and drug-likeness of compounds **6l** and **6m**

In view of the acceptable cytotoxicity of compounds **6l-m** against the tested cancer cell lines, molecular properties of designed compounds **6l-m** were calculated online using the free molecular calculation services provided by Molsoft (http://molsoft.com/mprop). As shown in Table 3, compounds **6l-m** showed acceptable molecular and drug-likeness properties.

Table 3 Molecular properties and drug-likeness of compounds **6l-m** [a]

Compound	MW	HBA	HBD	MolLogP	MolPSA (A^2)	MV (A^3)	Drug-likeness score
Desirable value	**<500**	**<10**	**<5**	**<5**	**<140**	---	About 1.0
6l	607.20	9	2	5.84	94.80	589.99	1.08
6m	523.12	7	2	5.68	72.84	493.09	0.69

[a] MW: Molecular weight; HBA: Number of hydrogen bond acceptors; HBD: Number of hydrogen bond donors; MolLogP: LogP value predicted by molsoft; MolPSA: Topological polar surface area; MV: Molecular volume.

2.4. LSD1 inactivation and molecular docking studies

Following our previously success in identifying LSD1 inhibitors for cancer therapy, we also tested the inhibitory ability of compounds **5a-p** and **6a-m** against LSD1 using the previously established methods [23-26]. **GSK2879552** was used as the control. As shown in Table 4, most of the compounds were found to be inactive toward LSD1. However, compounds **5p**, **5q**, and **6i** showed good inhibition against LSD1 with the IC_{50} values of 0.154, 1.19 and 0.557 μM, respectively. In contrast, compound **5a** with an amine group was inactive toward LSD1 (IC_{50} > 10 μM), highlighting the importance of the hydrazide group for the LSD1 inactivation. From the structural point of view, we can find that compounds **5p**, **5q**, and **6i** had similar structural feature - a hydrophilic group attached to the parent scaffold, which is consistent with our previous findings [23]. It is also worth noting that compound **5p** showed very potent inhibition against LSD1, but was almost inactive toward LSD1 overexpressed MGC-803 cells.

This finding may provide further evidence that LSD1 inactivation, at least for MGC-803 cells, is not directly correlated with growth inhibition of cancer cells.

Table 4 Inhibitory activity of compounds **5a-p** and **6a-m** against LSD1

Compound	LSD1 (IC_{50}/μM)	Compound	LSD1 (IC_{50}/μM)
5a	>10	**5q**	1.19±0.08
5b	>10	**6a**	>10
5c	>10	**6b**	>10
5d	>10	**6c**	>10
5e	>10	**6d**	>10
5f	>10	**6e**	>10
5g	>10	**6f**	>10
5h	>10	**6g**	>10
5i	>10	**6h**	>10
5j	>10	**6i**	0.557±0.006
5k	>10	**6j**	>10
5l	>10	**6k**	>10
5m	>10	**6l**	>10
5n	>10	**6m**	>10
5o	>10	**GSK2879552**	0.024
5p	0.154±0.002		

Docking simulations of compounds **5a**, **5p**, **5q**, and **6i** in the active site of LSD1 were performed to rationalize the potency using the MOE2014 software (PDB code: 2H94). The binding pose of the most potent compound **5p** in the active site of LSD1 is shown in Fig. 2A and 2B. Val333 formed multiple arene-H interactions with the [1,2,4]triazolo[1,5-a] pyrimidine scaffold, which also formed hydrogen bonds with surrounding Ala331 and Met332 residues. Besides, the NH_2 of the amino thiourea group also formed hydrogen bonds with Ala539 residue. In contrast, compound **5a** (LSD1 IC_{50} > 10 μM) did not show interactions with surrounding key residues (Fig. 2C). As shown in Fig. 2D, the binding pose of compound **5a** (highlighted in yellow) in the active site did not overlay with those of compounds **5p**, **5q**, and **6i** (highlighted in green, cyan, and red, respectively), while compounds **5p**, **5q**, and **6i** occupied the similar region. The docking results may explain the difference of the activity.

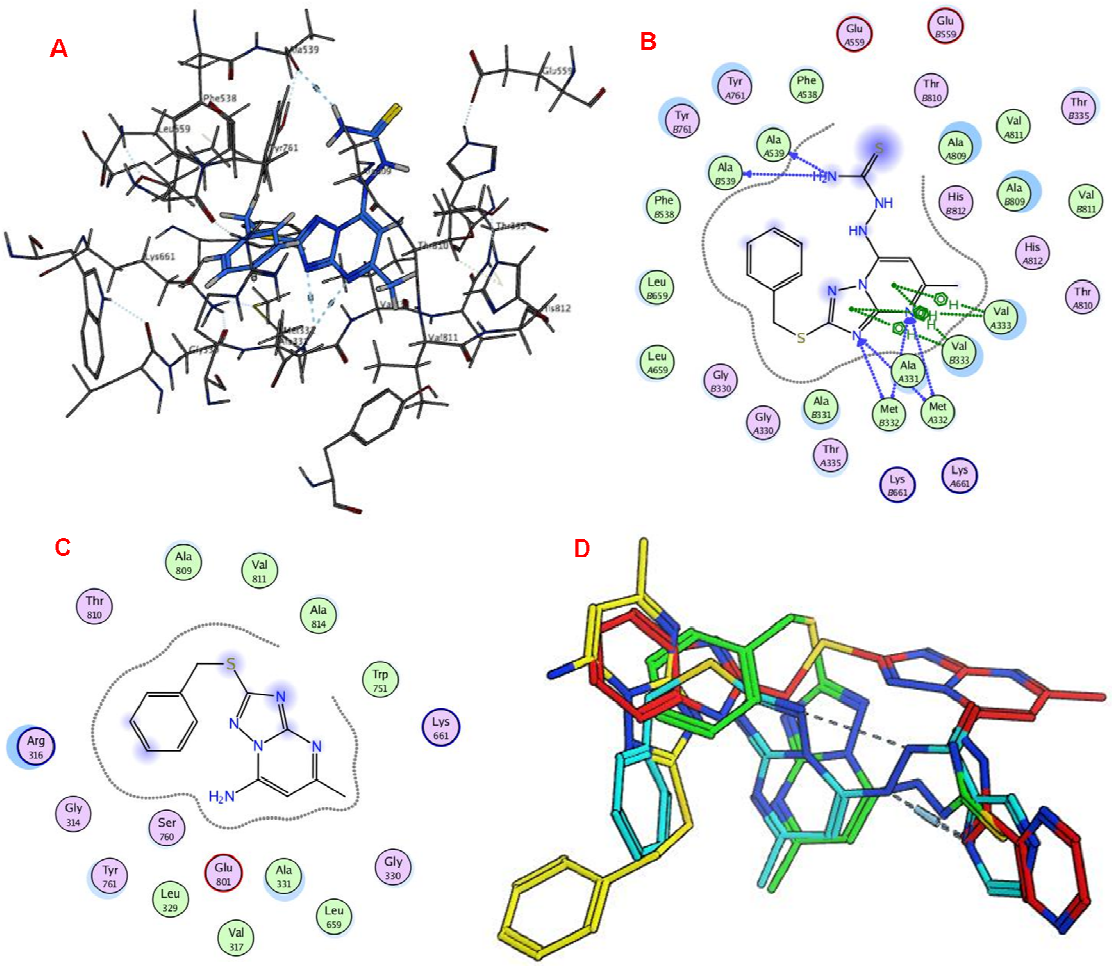

Fig.2 Predicted binding modes of compounds of interest in the active site of LSD1 (PDB code: 2H94). (A-B) 3D and 2D binding models of compound **5p** in the active site; (C) The binding pose of compound **5a** in the active site; (D) Overlay of four ligands, compounds **5a**, **5p**, **5q** and **6i** were highlighted in yellow, green, cyan and red respectively.

2.5. Migration inhibition of compound **5p** against MGC-803 and PC-9 cells

Recent studies have showed that LSD1 is associated with the migration and evasion of cancer cells, LSD1 overexpression promotes migration and evasion of tumor cells [34,35]. In MGC-803 and PC-9 cells, LSD1 has been reported to be overexpressed. Therefore, we explored the effect of compound **5p** (LSD1 IC_{50} = 154 nM) on the migration of MGC-803 and PC-9 cells. As shown in Fig. 3, compound **5p** significantly inhibited migration of MGC-803 cells in a concentration-dependent manner, especially at 10 μM, although compound **5p** showed 2.1% inhibition of MGC-803 cells at 10 μM (Table 1). This finding may offer further evidence that LSD1 inactivation causes migration of cancer cells, but cannot lead to the

growth inhibition. Intriguingly, compound **5p** did not affect the expression of the transmembrane proteins E-cadherin and N-cadherin in MGC-803 cells (Fig. 3).

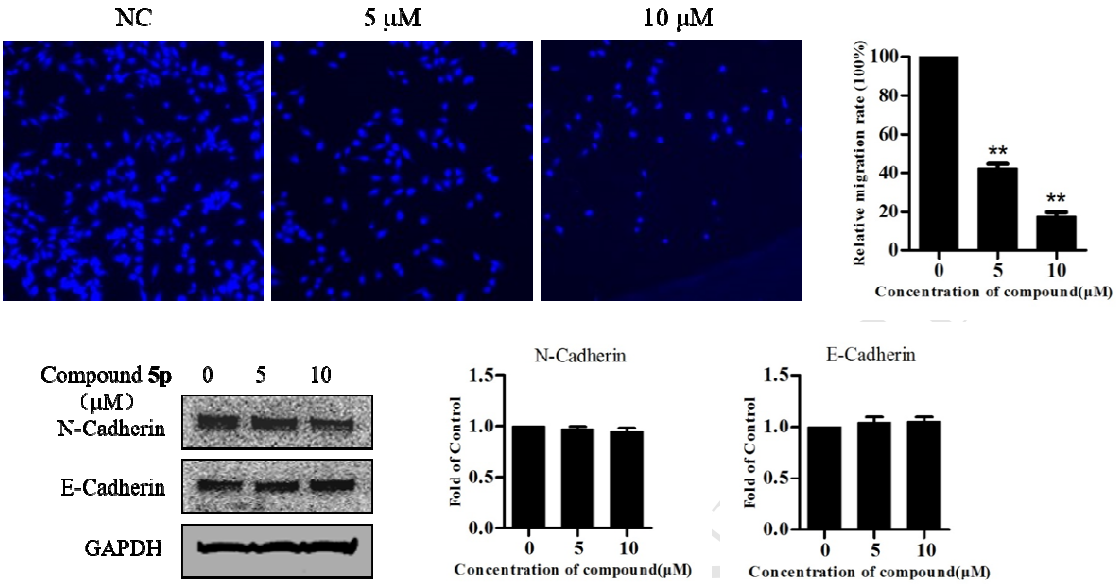

Fig. 3 The effect of compound **5p** on the migration of MGC-803 cells and expression levels of key proteins. $^{**}p < 0.01$.

Inspired by above observations, we further investigated the effect of compound **5p** on the migration of PC-9 cells. Similarly, compound **5p** concentration-dependently inhibited migration of PC-9 cells and also led to expression changes of E-cadherin and N-cadherin. Specifically, compound **5p** increased expression of E-cadherin, accompanied with decreased expression of N-cadherin (Fig. 4). The detailed mechanisms for the difference in MGC-803 and PC-9 cells need to be investigated further.

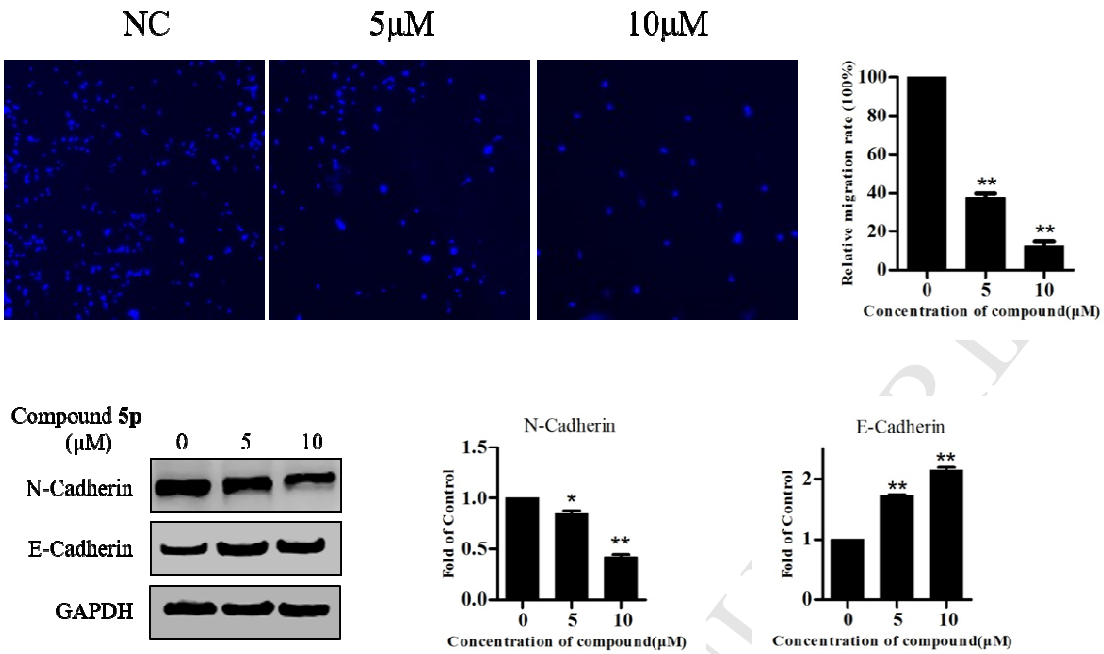

Fig. 4 The effect of compound **5p** on the migration of PC-9 cells and expression levels of key proteins. $^{**}p < 0.01$; $^{*}p < 0.01$.

3. Conclusions

Following our previous success in identifying LSD1 inhibitors for cancer therapy, we designed and synthesized a new series of [1,2,4]triazolo[1,5-a]pyrimidine-based LSD1 inhibitors, some of which showed potent inhibition toward LSD1 and selectively inhibited growth of A549 and PC-9 cells. Among these compounds, compound **6l** potently inhibited growth of PC-9 cells with an IC_{50} value of 0.59 μM, about 4-fold more potent than 5-FU. Further SARs studies led to the identification of compounds **6l-m** combining the chalcone and [1,2,4]triazolo[1,5-a] pyrimidine scaffold, which had good growth inhibition against all the tested cancer cell lines and were more potent than 5-FU and **GSK2879552**. Besides, compounds **5p**, **5q** and **6i** were found to be able to inhibit LSD1 potently with the IC_{50} values of 0.154, 1.19 and 0.557 μM, respectively. Docking studies of compound **5p** in the active site of LSD1 revealed that compound **5p** formed arene-H interactions with Val333 and hydrogen bonds with surrounding Ala331, Met332, and Ala539 residues. The in silico prediction also revealed the key motifs for LSD1 inactivation. Compound **5p** significantly inhibited migration of A549 and PC-9 cells in a concentration-dependent manner, but had remarkably different effect on the expression of transmembrane proteins (E-cadherin and N-cadherin). The exact mechanisms

for the difference induced by compound **5p** remain elusive and need to be investigated further. Our studies may provide further evidence that LSD1 inactivation is directly associated with the migration inhibition of cancer cells, not the growth inhibition. Taken together, our data may suggest that the [1,2,4]triazolo[1,5-a]pyrimidine scaffold can serve as a starting point for developing potent LSD1 inhibitors for cancer therapy.

4. Experimental section

4.1. General

Reagents and solvents were purchased from commercial sources and were used without further purification. Thin-layer chromatography (TLC) was carried out on glass plates coated with silica gel and visualized by UV light (254 nm). The products were purified by column chromatography over silica gel (200-300 mesh). Melting points were determined on a X-5 micromelting apparatus and are uncorrected. All the NMR spectra were recorded with a Bruker DPX 400 MHz spectrometer with TMS as an internal standard in $CDCl_3$ or DMSO-d_6. Chemical shifts are given as δ ppm values relative to TMS. High-resolution mass spectra (HRMS) were recorded on a Waters micromass Q-T of micromass spectrometer.

4.2. Synthesis of compounds **2a-b**

To a solution of 3-amino-5-mercapto-1,2,4-triazole (1.0 g) in acetone (30 mL) were added sodium carbonate (1.37 g, 12.92 mmol), sodium iodide (129.06 mg, 0.861 mmol) and benzyl bromide (1.13 mL, 9.47 mmol) or 2-(chloromethyl)-1*H*-benzo[*d*]imidazole (1.58 g, 9.47 mmol). The reaction mixture was stirred at 60 ^{o}C for 3-6 h before cooling to room temperature. Na_2CO_3 and NaI were removed via filtration. The residue was concentrated under vacuum and then dissolved in EtOAc. The organic layer was washed with water (2 × 10 mL) and brine (2 × 20 mL) and then dried over $MgSO_4$. After removal of the solvent, the resulting residue was subjected to column chromatography, giving the corresponding products **2a** and **2b**.

Compound **2a**, white solid (1.3 g), yield: 73.2%. ^{1}H NMR (400 MHz, DMSO-d_6) δ 7.41-7.18 (m, 5H), 4.34 (s, 2H). ^{13}C NMR (100 MHz, DMSO-d_6) δ 152.19, 147.08, 136.55, 128.79, 128.43, 127.48, 35.41. HRMS (ESI): m/z calcd for $C_9H_9N_4S$ $(M-H)^-$, 205.0548; found, 205.0548.

Compound **2b**, white solid, yield: 60%. ^{1}H NMR (400 MHz, DMSO- d_6) δ 12.30 -12.08 (brs, 2H), 7.50 (m, 2H), 7.25-6.99 (m, 2H), 6.14 (s, 2H), 4.45 (s, 2H). HRMS (ESI): m/z calcd for $C_{10}H_9N_6S$ $(M-H)^-$, 245.0609; found, 245.0609.

4.3. Synthesis of compounds **3a-b**

Compound **2a** or **2b** (1g, 1.0 eq) and ethyl acetoacetate (1.0 eq) were dissolved in AcOH (10 mL) and the solution was kept at 120 ^{o}C for about 3-6 h. Upon completion of the reaction, the mixture was cooled to room temperature; the formed white precipitate was filtered, washed with water and dried under vacuum to afford the desired compound **3a** or **3b**.

Compound **3a**, white solid (1.12 g), yield: 85%. m.p.: 240-245 ^{o}C. ^{1}H NMR (400 MHz, DMSO-d_6) δ 13.17 (s, 1H), 7.44 (d, J = 7.1 Hz, 2H), 7.32 (t, J = 7.3 Hz, 2H), 7.26 (d, J = 7.2 Hz, 1H), 5.80 (s, 1H), 4.43 (s, 2H), 2.29 (s, 3H). ^{13}C NMR (100MHz, DMSO-d_6) δ 161.92, 154.75, 151.09, 150.63, 137.35, 128.77, 128.38, 127.22, 98.46, 34.48, 18.43. HRMS (ESI): m/z calcd for $C_{13}H_{11}N_4OS$ $(M-H)^-$, 271.0654; found, 271.0660.

Compound **3b**, white solid (1.1 g), yield: 88%. m.p.: 196-209 ^{o}C. ^{1}H NMR (400 MHz, DMSO-d_6) δ 12.76 (s, 2H), 7.50 (dd, J = 5.9, 3.2 Hz, 2H), 7.15 (dd, J = 6.0, 3.1 Hz, 2H), 5.81 (s, 1H), 4.68 (s, 2H), 2.29 (s, 3H). ^{13}C NMR (100 MHz, DMSO-d_6) δ 161.41, 154.85, 151.36, 150.91, 150.21, 121.76, 98.55, 28.46, 18.58. HRMS (ESI): m/z calcd for $C_{14}H_{11}N_6OS$ $(M-H)^-$, 311.0715; found, 311.0723.

4.4. Synthesis of compounds **4a-b**

The solution of compound **3a** or **3b** in $POCl_3$ (excess) was kept at 90 ^{o}C for 3-5 h. Upon completion of the reaction, the mixture was added dropwise to the crushed ice. The resulting aqueous mixture was extracted with CH_2Cl_2 (4 × 30 mL) and the organic layers were washed with saturated aqueous $NaHCO_3$ (3 × 10 mL), dried over $MgSO_4$ and concentrated under reduced pressure to give compounds **4a-b**. However, compounds **4a**-**b** were unstable and therefore only characterized by HRMS (please see the supporting information for HRMS spectra).

4.5. General procedure for the synthesis of compounds **5a-k**, **5m-q** and **6a-m**

Compound **4a** or compound **4b** (1.0 eq) was dissolved in ethanol (2 mL) and then the corresponding amine derivative (1.0 eq) was added. The reaction mixture was stirred at room temperature until the reaction was done (monitored by TLC). The resultant mixture was concentrated under reduced pressure and purified by column chromatography to give the corresponding product.

Compound **5a**, yellow solid, yield: 89%. m.p.: 196-201 ^{o}C. ^{1}H NMR (400 MHz, DMSO-d_6) δ 7.93 (s, 2H), 7.55-7.43 (m, 2H), 7.37-7.28 (m, 2H), 7.24 (dd, *J* = 8.4, 6.1 Hz, 1H), 6.12 (s, 1H), 4.49 (s, 2H), 2.37 (s, 3H). ^{13}C NMR (100 MHz, DMSO-d_6) δ 164.29, 162.84, 155.87, 147.50, 138.07, 128.92, 128.38, 127.16, 90.25, 34.36, 24.37. HRMS (ESI): m/z calcd for $C_{13}H_{12}N_5S$ $(M-H)^-$, 270.0813; found, 270.0821.

Compound **5b**, white solid, yield: 89%. m.p.: 189-192 ^{o}C . ^{1}H NMR (400 MHz, $CDCl_3$) δ 7.71 (s, 1H), 7.51-7.44 (m, 4H), 7.36-7.27 (m, 5H), 7.26-7.20 (m, 1H), 6.30 (s, 1H), 4.54 (s, 2H), 2.51 (s, 3H). ^{13}C NMR (100 MHz, $CDCl_3$) δ 166.54, 164.77, 155.92, 144.35, 137.57, 135.76, 130.02, 129.11, 128.53, 127.36, 126.92, 123.82, 89.01, 35.80, 25.41. HRMS (ESI): m/z calcd for $C_{19}H_{16}N_5S$ $(M-H)^-$, 346.1126; found, 346.1135.

Compound **5c**, white solid, yield: 89%. m.p.: 240-247 ^{o}C. ^{1}H NMR (400 MHz, DMSO-d_6) δ 11.03 (s, 1H), 7.51 (d, *J* = 6.1 Hz, 2H), 7.30 (s, 7H), 6.36 (s, 1H), 4.57 (s, 2H), 2.45 (s, 3H), 2.36 (s, 3H). ^{13}C NMR (100 MHz, DMSO-d_6) δ 165.10, 159.74, 152.19, 146.52, 137.51, 136.70, 132.89, 130.08, 128.88, 128.41, 127.29, 124.97, 90.27, 34.51, 21.74, 20.54. HRMS (ESI): m/z calcd for $C_{20}H_{18}N_5S$ $(M-H)^-$, 360.1283; found, 360.1292.

Compound **5d**, yellow solid, yield: 92%. m.p.: 227-231 ^{o}C.^{1}H NMR (400 MHz, DMSO-d_6) δ 11.01 (s, 1H), 7.49 (m, 4H), 7.41-7.22 (m, 5H), 6.37 (s, 1H), 4.57 (s, 2H), 2.45 (s, 3H). ^{13}C NMR (100 MHz, DMSO-d_6) δ 165.20, 161.90, 160.23, 159.47, 152.44, 146.64, 137.60, 132.00, 128.95, 128.48, 127.50(*J* = 8 Hz), 127.36, 116.54(*J* = 23 Hz), 90.38, 34.58, 22.00. HRMS (ESI): m/z calcd for $C_{19}H_{15}FN_5S$ $(M-H)^-$, 364.1032; found, 364.1041.

Compound **5e**, white solid, yield: 79%. m.p.: 196-207 ^{o}C. ^{1}H NMR (400 MHz, DMSO-d_6) δ 9.95 (s, 1H), 7.48 (d, *J* = 7.2 Hz, 2H), 7.32 (t, *J* = 7.4 Hz, 2H), 7.26 (d, *J* = 7.2 Hz, 1H), 6.76 (s, 2H), 6.40 (s, 1H), 4.54 (s, 2H), 3.78 (s, 6H), 3.69 (s, 3H), 2.40 (s, 3H). ^{13}C NMR (100MHz, DMSO-d_6)

δ 164.46, 164.00, 155.76, 153.24, 145.14, 138.02, 135.67, 132.32, 128.90, 128.43, 127.21, 102.55, 89.64, 60.08, 56.02, 34.49, 24.66. HRMS (ESI): m/z calcd for $C_{22}H_{22}N_5O_3S$ $(M-H)^-$, 436.1443; found, 436.1451.

Compound **5f**, yellow solid. Yield: 93%. m.p.: 186-190 °C. ^{1}H NMR (400 MHz, DMSO-d_6) δ 12.89 (s, 1H), 10.32 (s, 1H), 8.02 (d, *J* = 8.6 Hz, 2H), 7.57 (d, *J* = 8.5 Hz,2H), 7.49 (d, *J* = 7.2 Hz, 2H), 7.32 (t, *J* = 7.4 Hz, 2H), 7.25 (t, *J* = 7.2 Hz, 1H), 6.62 (s, 1H), 4.56 (s, 2H), 2.44 (s, 3H). ^{13}C NMR (100 MHz, DMSO-d_6) δ 166.69, 164.70, 164.32, 155.79, 143.96, 141.24, 137.94, 130.68, 128.89, 128.43, 127.30, 127.23, 122.76, 90.48, 34.57, 24.71. HRMS (ESI): m/z calcd for $C_{20}H_{16}N_5O_2S$ $(M-H)^-$, 390.1025; found, 390.1036.

Compound **5g**, white solid, yield: 89%. m.p.: 204-207 °C. ^{1}H NMR (400 MHz, DMSO-d_6) δ 7.45 (d, *J* = 7.2 Hz, 2H), 7.32 (t, *J* = 7.4 Hz, 2H), 7.24 (t, *J* = 7.3 Hz, 1H), 6.50 (s, 1H), 4.45 (s, 2H), 3.77 (s, 4H), 3.75 (s, 4H), 2.45 (s, 3H). ^{13}C NMR (100 MHz, DMSO-d_6) δ 164.01, 163.91, 157.00, 148.66, 137.90, 128.73, 128.34, 127.13, 94.33, 65.49,s 47.76, 34.39, 24.48. HRMS (ESI): m/z calcd for $C_{17}H_{20}N_5OS$ $(M + H)^+$, 342.1389; found, 342.1381.

Compound **5h**, yellow solid, yield: 76%. m.p.: 173-176 °C. ^{1}H NMR (400 MHz, DMSO-d_6) δ 7.46 (d, *J* = 7.2 Hz, 2H), 7.31 (t, *J* = 7.4 Hz, 2H), 7.24 (t, *J* = 7.3 Hz, 1H), 6.46 (s, 1H), 4.45 (s, 2H), 3.67 (t, *J* = 4 Hz, 4H), 2.86 (m, *J* = 4 Hz, 4H), 2.43 (s, 3H). ^{13}C NMR (100 MHz, DMSO-d_6) δ 169.05, 168.97, 162.35, 154.11, 143.21, 134.00, 133.57, 132.37, 99.52, 54.04, 50.30, 39.61, 29.71. HRMS (ESI): m/z calcd for $C_{17}H_{21}N_6S$ $(M + H)^+$, 341.1548; found, 341.1542.

Compound **5i**, yellow solid, yield: 77%. m.p.: 136-142 °C. ^{1}H NMR (400 MHz, DMSO-d_6) δ 7.46 (d, *J* = 7.2 Hz, 2H), 7.32 (t, *J* = 7.4 Hz, 2H), 7.24 (t, *J* = 7.3 Hz, 1H), 6.48 (s, 1H), 4.48 (s, 1H), 4.45 (s, 2H), 3.75 (d, *J* = 4.5 Hz, 4H), 3.55 (d, *J* = 3.0 Hz, 2H), 2.62 (d, *J* = 4.5 Hz, 4H), 2.47 (t, *J* = 6.1 Hz, 2H), 2.44 (s, 3H). ^{13}C NMR (100 MHz, DMSO-d_6) δ 163.89, 163.77, 157.06, 148.64, 137.93, 128.77, 128.33, 127.13, 94.40, 59.98, 58.47, 52.44, 47.46, 34.37, 24.46. HRMS (ESI): m/z calcd for $C_{19}H_{25}N_6OS$ $(M + H)^+$, 385.1811; found, 385.1802.

Compound **5j**, yellow solid, yield: 71%. m.p.: 186-189 °C. ^{1}H NMR (400 MHz, $CDCl_3$) δ 7.44 (d, *J* = 7.2 Hz, 2H), 7.28 (d, *J* = 7.0 Hz, 2H), 7.21 (t, *J* = 7.3 Hz, 1H), 6.03 (s, 1H), 4.47 (s, 2H), 3.14 (s, 1H), 2.97 (m, 6H), 2.50 (s, 3H), 2.29 (d, *J* = 12.0 Hz, 2H), 2.00-1.83 (m, 6H), 1.58 (s, 2H). ^{13}C

NMR (100 MHz, $CDCl_3$) δ 165.89, 164.46, 157.48, 148.64, 137.57, 128.99, 128.52, 127.34, 94.52, 62.96, 50.00, 47.14, 35.57, 26.18, 25.11, 23.89, 23.17. HRMS (ESI): m/z calcd for $C_{23}H_{31}N_6S$ $(M + H)^+$, 423.2331; found, 423.2323.

Compound **5k**, white solid, yield: 85%. m.p.: 193-196 °C. ^{1}H NMR (400 MHz, DMSO-d_6) δ 8.36 (t, *J* = 5.7 Hz, 1H), 7.51-7.42 (m, 2H), 7.35-7.28 (m, 2H), 7.27-7.20 (m, 1H), 6.30 (s, 1H), 4.50 (s, 2H), 3.61 (t, *J* = 4.5 Hz, 4H), 3.42 (q, *J* = 6.3 Hz, 2H), 2.45-2.29 (m, 9H), 1.78 (m, 2H). ^{13}C NMR (100 MHz, DMSO-d_6) δ 163.98, 163.29, 155.48, 146.31, 137.87, 128.79, 128.34, 127.12, 87.75, 65.96, 55.93, 53.21, 40.56, 34.38, 24.62, 24.38. HRMS (ESI): m/z calcd for $C_{20}H_{27}N_6OS$ $(M + H)^+$, 399.1967; found, 399.1960.

Compound **5m**, white solid. Yield: 74%. m.p.: 199-203 °C. ^{1}H NMR (400 MHz, DMSO-d_6) δ 8.07 (t, *J* = 6.0 Hz, 1H), 7.47 (d, *J* = 7.2 Hz, 2H), 7.31 (t, *J* = 7.3 Hz, 2H), 7.25 (d, *J* = 7.2 Hz, 1H), 6.29 (s, 1H), 4.62 (t, *J* = 4.9 Hz, 1H), 4.49 (s, 2H), 3.51 (m, 2H), 3.42 (m, 2H), 2.41 (s, 3H), 1.84 – 1.69 (m, 2H). ^{13}C NMR (100 MHz, DMSO-d_6) δ 163.94, 163.35, 155.52, 146.28, 137.96, 128.85, 128.32, 127.10, 87.71, 58.25, 34.38, 31.22, 24.62. HRMS (ESI): m/z calcd for $C_{16}H_{20}N_5OS$ $(M + H)^+$, 330.1389; found, 330.1379.

Compound **5n**, white solid, yield: 90%. m.p.: 203-207 °C. ^{1}H NMR (400 MHz, DMSO-d_6) δ 10.83 (s, 1H), 8.13 (t, *J* = 6.1 Hz, 1H), 7.59 (d, *J* = 7.8 Hz, 1H), 7.46 (d, *J* = 7.1 Hz, 2H), 7.38-7.28 (m, 3H), 7.23 (m, 2H), 7.07 (t, *J* = 8, 4.0 Hz, 1H), 6.98 (t, *J* = 7.4 Hz, 1H), 6.18 (s, 1H), 4.49 (s, 2H), 3.65 (m, 2H), 3.06 (t, *J* = 7.2 Hz, 2H), 2.32 (s, 3H). ^{13}C NMR (100 MHz, DMSO-d_6) δ 163.91, 163.17, 146.23, 137.95, 136.15, 128.83, 128.33, 127.11, 123.03, 120.90, 118.21, 118.10, 111.28, 110.90, 87.84, 42.18, 34.37, 24.49, 24.43, 13.99. HRMS (ESI): m/z calcd for $C_{23}H_{23}N_6S$ $(M + H)^+$, 415.1705; found, 415.1696.

Compound **5o**, white solid, yield: 91%. m.p.: 209-213 °C. ^{1}H NMR (400 MHz, DMSO-d_6) δ 8.23 (t, *J* = 6.0 Hz, 1H), 7.67 (s, 1H), 7.52-7.42 (m, 2H), 7.31 (m, 2H), 7.25 (m, 1H), 7.22 (s, 1H), 6.91 (s, 1H), 6.20 (s, 1H), 4.50 (s, 2H), 4.06 (t, *J* = 7.0 Hz, 2H), 3.33 (m, 2H), 2.41 (s, 3H), 2.06 (p, *J* = 6.9 Hz, 2H). ^{13}C NMR (100 MHz, DMSO-d_6) δ 163.96, 163.39, 155.52, 146.23, 137.96, 137.25, 128.83, 128.32, 127.11, 119.25, 87.79, 43.48, 34.39, 29.69, 24.61. HRMS (ESI): m/z calcd for $C_{19}H_{22}N_7S$ $(M + H)^+$, 380.1657; found, 380.1649.

Compound **5p**, yellow solid, yield: 92%. m.p.: 227-231 °C. ^{1}H NMR (400 MHz, DMSO-d_6) δ 10.39 (s, 1H), 9.78 (s, 1H), 8.15 (s, 1H), 7.91 (s, 1H), 7.49 (d, *J* = 7.3 Hz, 2H), 7.31 (t, *J* = 7.3 Hz, 2H), 7.25 (t, *J* = 7.3 Hz, 1H), 6.09 (s, 1H), 4.51 (s, 2H), 2.45 (s, 3H). ^{13}C NMR (100 MHz, DMSO-d_6) δ 182.14, 164.60, 163.82, 155.69, 147.09, 138.02, 128.84, 128.31, 127.10, 88.32, 34.25, 24.64. HRMS (ESI): m/z calcd for $C_{14}H_{14}N_7S_2$ $(M-H)^-$, 344.0752; found, 344.0760.

Compound **5q**, yellow solid, yield: 90%. m.p.: 196-200 °C. 1H NMR (400 MHz, DMSO-d_6) δ 11.38 (s, 1H), 10.45 (s, 1H), 9.25 (d, J = 1.2 Hz, 1H), 8.96 (s, 1H), 8.83 (s, 1H), 7.51 (d, J = 7.1 Hz, 3H), 7.32 (t, J = 7.3 Hz, 2H), 7.26 (t, J = 7.3 Hz, 1H), 6.36 (s, 1H), 4.55 (s, 2H), 2.40 (s, 3H). ^{13}C NMR (100 MHz, DMSO-d_6) δ 148.19, 143.96, 143.58, 137.91, 128.93, 128.44, 127.25, 34.41. HRMS (ESI): m/z calcd for $C_{18}H_{17}N_8OS$ $(M + H)^+$, 393.1246; found, 393.1235.

Compound **6a**, white solid, yield: 79%. m.p.: 180-19 °C. ^{1}H NMR (400 MHz, DMSO-d_6) δ 10.15 (s, 1H), 7.50 (m, 6H), 7.33 (d, *J* = 7.0 Hz, 1H), 7.18 (dd, *J* = 6.0, 3.1 Hz, 2H), 6.34 (s, 1H), 4.79 (s, 2H), 2.38 (s, 3H). ^{13}C NMR (100 MHz, DMSO-d_6) δ 164.03, 163.80, 155.80, 150.66, 144.94, 136.53, 129.48, 126.12, 124.44, 122.01, 114.75, 89.29, 28.00, 24.60. HRMS (ESI): m/z calcd for $C_{20}H_{16}N_7S$ $(M-H)^-$, 386.1188; found, 386.1196.

Compound **6b**, white solid, yield: 86%. m.p.: 240-247 °C. ^{1}H NMR (400 MHz, DMSO-d_6) δ 11.41 (s, 1H), 7.79 (s, 2H), 7.53 (s, 2H), 7.37 (t, *J* = 6.7 Hz, 4H), 6.37 (s, 1H), 5.09 (s, 2H), 2.41 (s, 3H), 2.37 (s, 3H). ^{13}C NMR (100 MHz, DMSO-d_6) δ 163.37, 152.43, 150.23, 146.66, 136.98, 132.59, 130.62, 130.10, 125.96, 125.35, 125.17, 113.96, 90.51, 25.10, 21.51, 20.64. HRMS (ESI): m/z calcd for $C_{21}H_{18}N_7S$ $(M-H)^-$, 400.1344; found, 400.1352.

Compound **6c**, white solid, yield: 91%. m.p.: 207-215 °C. ^{1}H NMR (400 MHz, DMSO-d_6) δ 7.63 (dd, *J* = 6.0, 3.1 Hz, 2H), 7.49 (dd, *J* = 8.8, 4.9 Hz, 2H), 7.40-7.25 (m, 4H), 6.27 (s, 1H), 4.88 (s, 2H), 2.37 (s, 3H). ^{13}C NMR (100 MHz, DMSO-d_6) δ 164.13, 163.35, 161.32, 158.90, 155.72, 150.82, 145.29, 134.10 (*J* = 248 Hz), 127.05 (*J* = 9 Hz), 123.35, 116.30 (*J* = 22 Hz), 114.48, 89.29, 27.21, 24.54. HRMS (ESI): m/z calcd for $C_{20}H_{15}FN_7S$ $(M-H)^-$, 404.1094; found, 404.1102.

Compound **6d**, white solid, yield: 81%. m.p.: 213-217 °C. ^{1}H NMR (400 MHz, DMSO-d_6) δ 7.79 (dd, *J* = 6.1, 3.1 Hz, 2H), 7.54 (m, 6H), 6.45 (s, 1H), 5.07 (s, 2H), 2.39 (s, 3H). ^{13}C NMR (100 MHz, DMSO-d_6) δ 163.11, 161.84, 153.87, 150.47, 145.79, 134.79, 131.02, 130.63, 129.53,

126.89, 125.94, 113.95, 90.39, 25.12, 22.77. HRMS (ESI): m/z calcd for $C_{20}H_{15}ClN_7S$ $(M-H)^-$, 420.0798; found, 420.0808.

Compound **6e**, white solid, yield: 78%. m.p.: 289-292 ^oC. ^1H NMR (400 MHz, DMSO-d_6) δ 12.43 (s, 1H), 10.18 (s, 1H), 7.66 (d, *J* = 8.7 Hz, 2H), 7.55-7.46 (m, 2H), 7.42 (d, *J* = 8.7 Hz, 2H), 7.15 (dd, *J* = 6.0, 3.2 Hz, 2H), 6.42 (s, 1H), 4.77 (s, 2H), 2.40 (s, 3H). ^{13}C NMR (100 MHz, DMSO-d_6) δ 164.24, 164.06, 155.84, 150.61, 144.67, 136.19, 132.38, 126.38, 121.74, 118.26, 89.70, 28.34, 24.66. HRMS (ESI): m/z calcd for $C_{20}H_{16}BrN_7S$ $(M-H)^-$, 400.1344; found, 400.1352.

Compound **6f**, white solid, yield: 89%. m.p.: 236-239 ^oC. ^1H NMR (400 MHz, DMSO-d_6) δ 7.96 (d, *J* = 8.6 Hz, 2H), 7.83-7.70 (m, 4H), 7.51 (dd, *J* = 6.1, 3.1 Hz, 2H), 6.68 (s, 1H), 5.08 (s, 2H), 2.42 (s, 3H). ^{13}C NMR (100 MHz, DMSO-d_6) δ 163.02, 154.48, 150.51, 144.49, 140.88, 133.59, 130.55, 125.86, 124.23, 118.54, 113.88, 107.87, 91.25, 25.04, 23.34.
HRMS (ESI): m/z calcd for $C_{21}H_{15}N_8S$ $(M-H)^-$, 411.1140; found, 411.1149.

Compound **6g**, pink Solid, yield: 85%. m.p.:230-235 ^oC. ^1H NMR (400 MHz, DMSO-d_6) δ 8.05 (d, *J* = 8.5 Hz, 2H), 7.80 (dd, *J* = 6.1, 3.1 Hz, 2H), 7.66 (d, *J* = 8.5 Hz, 2H), 7.52 (dd, *J* = 6.1, 3.1 Hz, 2H), 6.63 (s, 1H), 5.09 (s, 2H), 2.42 (s, 3H). ^{13}C NMR (100 MHz, DMSO-d_6) δ 166.64, 163.04, 162.70, 154.38, 150.60, 145.01, 140.26, 130.67, 130.64, 128.25, 125.94, 123.94, 113.96, 90.88, 25.15, 23.25. HRMS (ESI): m/z calcd for $C_{21}H_{16}N_7O_2S$ $(M-H)^-$, 430.1086; found, 430.1094.

Compound **6h**, white solid, yield: 88%. m.p.: 228-235 ^oC. ^1H NMR (400 MHz, DMSO-d_6) δ 7.80 (dd, *J* = 6.2, 3.1 Hz, 2H), 7.53 (dd, *J* = 6.2, 3.1 Hz, 2H), 6.84 (s, 2H), 6.52 (s, 1H), 5.08 (s, 2H), 3.81 (s, 6H), 3.72 (s, 3H), 2.41 (s, 3H). ^{13}C NMR (100 MHz, DMSO-d_6) δ 163.05, 153.24, 150.54, 145.99, 136.19, 131.32, 130.66, 125.93, 113.97, 103.01, 90.51, 60.09, 56.07, 25.16, 22.84.
HRMS (ESI): m/z calcd for $C_{23}H_{22}N_7O_3S$ $(M-H)^-$, 476.1505; found, 476.1513.

Compound **6i**, green solid, yield: 94%. m.p.: 187-191 ^oC. ^1H NMR (400 MHz, DMSO-d_6) δ 11.47 (s, 1H), 9.26 (d, *J* = 1.2 Hz, 1H), 8.98 (d, *J* = 2.4 Hz, 1H), 8.85 (s, 1H), 7.78 (m, 2H), 7.60 -7.40 (m, 2H), 6.38 (s, 1H), 5.04 (s, 2H), 2.38 (s, 3H). ^{13}C NMR (100 MHz, DMSO-d_6) δ 164.27, 163.20, 162.69, 155.63, 150.72, 148.17, 147.17, 143.93, 143.80, 143.56, 131.14, 125.60,

390 113.98, 89.05, 25.54, 24.33. HRMS (ESI): m/z calcd for $C_{19}H_{15}N_{10}OS$ $(M-H)^-$, 431.1151; found,
391 431.1161.

392 Compound **6j**, white solid, yield: 82%. m.p.: 212-218 °C. ^{1}H NMR (400 MHz, DMSO-d_6) δ 10.96
393 (s, 1H), 7.81 (dd, *J* = 6.2, 3.2 Hz, 2H), 7.54 (m, 4H), 7.45 (d, *J* = 8.6 Hz, 2H), 6.49 (s, 1H), 5.09 (s,
394 2H), 2.54 (s, 1H), 2.41 (s, 4H), 2.26 (m, 2H), 2.02-1.82 (m, 2H), 0.82 (t, *J* = 7.3 Hz, 3H). ^{13}C
395 NMR (100 MHz, DMSO-d_6) δ 175.49, 172.69, 162.87, 162.30, 154.25, 150.59, 138.21, 134.75,
396 130.62, 127.40, 125.86, 124.84, 113.91, 90.06, 50.03, 32.00, 29.07, 26.01, 25.11, 23.14, 8.92.
397 HRMS (ESI): m/z calcd for $C_{27}H_{25}N_8O_2S$ $(M-H)^-$, 525.1821; found, 525.1831.

398 Compound **6k**, pink solid, yield: 94%. m.p.: 270-276 °C. ^{1}H NMR (400 MHz, DMSO-d_6) δ 11.07
399 (s, 1H), 7.91-7.67 (m, 5H), 7.54 (dd, *J* = 5.8, 2.9 Hz, 2H), 6.26-6.02 (m, 1H), 5.20 (dd, *J* = 13.1,
400 4.8 Hz, 1H), 5.07 (s, 2H), 4.58 (d, *J* = 17.6 Hz, 1H), 4.51 ((m, 2H), 3.03-2.83 (m, 1H), 2.60 (m,
401 1H), 2.35 (s, 3H), 2.31-2.16 (m, 1H), 2.03 (s, 1H). ^{13}C NMR (100 MHz, DMSO-d_6) δ 172.84,
402 170.90, 167.41, 163.11, 162.10, 154.05, 150.46, 146.06, 138.88, 133.73, 131.08, 130.67,
403 130.26, 129.86, 125.95, 122.69, 113.91, 90.26, 51.49, 45.78, 31.09, 25.17, 22.88, 22.63.
404 HRMS (ESI): m/z calcd for $C_{27}H_{22}N_9O_3S$ $(M-H)^-$, 552.1566; found, 552.1578.

405 Compound **6l**, yellow Solid, yield: 91%. m.p.: 224-226 °C. ^{1}H NMR (400 MHz, DMSO-d_6) δ
406 8.32 (d, *J* = 8.5 Hz, 2H), 7.96 (d, *J* = 15.5 Hz, 1H), 7.85-7.67 (m, 5H), 7.52 (dd, *J* = 6.0, 3.0 Hz,
407 2H), 7.26 (s, 2H), 6.69 (s, 1H), 5.09 (s, 2H), 3.88 (s, 6H), 3.72 (s, 3H), 2.43 (s, 3H). ^{13}C NMR
408 (100 MHz, DMSO-d_6) δ 187.75, 163.01, 154.66, 153.10, 150.66, 144.76, 144.48, 140.71,
409 139.80, 134.92, 130.67, 130.19, 130.05, 125.94, 123.70, 121.01, 113.96, 106.58, 91.08, 60.13,
410 56.15, 25.18, 23.48. HRMS (ESI): m/z calcd for $C_{32}H_{28}N_7O_4S$ $(M-H)^-$, 606.1923; found,
411 606.1936.

412 Compound **6m**, yellow Solid, yield: 87%. m.p.: 228-231 °C. ^{1}H NMR (400 MHz, DMSO-d_6) δ
413 8.23 (d, *J* = 8.6 Hz, 2H), 7.95 (d, *J* = 15.3 Hz, 1H), 7.82-7.76 (m, 3H), 7.76-7.69 (m, 3H), 7.62 (d,
414 *J* = 15.3 Hz, 1H), 7.52 (dd, *J* = 6.1, 3.1 Hz, 2H), 7.25-7.16 (m, 1H), 6.68 (s, 1H), 5.09 (s, 2H),
415 2.43 (s, 3H). ^{13}C NMR (100 MHz, DMSO-d_6) δ 187.31, 162.98, 154.47, 150.55, 144.77, 140.56,
416 139.64, 136.69, 134.77, 132.88, 130.58, 130.53, 129.81, 128.68, 125.87, 124.43, 123.78,

120.10, 113.89, 91.02, 25.08, 23.30. HRMS (ESI): m/z calcd for $C_{27}H_{20}N_7OS_2$ $(M-H)^-$, 522.1171; found, 522.1181.

4.6. Synthesis of compound **5l**

Compound **4a** (1eq) was dissolved in anhydrous tetrahydrofuran (2 mL), followed by addition of *t*-BuOK (1.5eq) and 2-(pyrrolidin-1-yl)ethan-1-ol (1.0 eq). The reaction mixture was stirred at room temperature for 10 h. The resultant mixture was concentrated under reduced pressure to give the residue, which was then purified by column chromatograph. Compound **5l**, yellow solid, yield: 69%. m.p.: 197-200 ^{o}C. ^{1}H NMR (400 MHz, $CDCl_3$) δ 7.51-7.42 (m, 2H), 7.32-7.25 (m, 2H), 7.25-7.19 (m, 1H), 6.25 (s, 1H), 4.53 (s, 2H), 4.49 (t, *J* = 6.1 Hz, 2H), 3.09 (t, *J* = 6.1 Hz, 2H), 2.75-2.63 (m, 4H), 2.62 (s, 3H), 1.90-1.76 (m, 4H). ^{13}C NMR (100 MHz, $CDCl_3$) δ 167.76, 166.15, 157.16, 154.17, 137.49, 129.17, 128.48, 127.32, 90.14, 70.10, 54.76, 53.78, 35.69, 29.70, 25.49, 23.61. HRMS (ESI): m/z calcd for $C_{19}H_{24}N_5OS$ $(M + H)^+$, 370.1702; found, 370.1695.

4.7. Biological testing

The MTT [32] and LSD1 inhibition [24] assay were carried out following our previously reported methods. Therefore, no details are given here.

4.8. Molecular docking studies

The protein complexes used for this study were obtained from protein data bank (PDB code: 2H94), and all water molecules were eliminated. Hydrogen and partial charges were added by the protonate 3D program of MOE2014; Energy minimization of the ligands was carried out using energy minimize program of MOE. Default parameter settings generated by the program of MOE were used for docking.

4.9. Transwell assay

For the migration assay, 100 μL medium containing 1% FBS, different concentrations of compound **5p** and 10, 000 cells were added to each upper chamber. In the lower chamber, 500 μL medium with 20% FBS was used as chemoattractant. After incubation for 24 h, both chambers were washed by PBS for three times. After staining with Hoechst 33258 (10 μg/mL)

444 and twice wash, migrated cells were detected and numbered using high content screening
445 system (ArrayScan XTI, Thermo Fisher Scientific, MA).

446 4.10. Western blot analysis

447 Cells were seeded and treated with 0, 5, and 10 μM of compound **5p** for 24 h, then cells were
448 collected and lysed by radio immunoprecipitation assay (RIPA) lysis buffer (50 mM Tris-HCl,
449 pH 7.5, 150 mM NaCl, 0.25% sodium deoxycholate, 0.1% Nonidet P-40, 0.1% Triton X-100)
450 with the complete proteinase inhibitor cocktail (Roche, Basel, Switzerland) for 30 min. After
451 centrifugation of 12,000 rpm for 10 min at 4˚C, supernatant was collected and the protein
452 concentration was detected using a bicinchonininc acid (BCA) assay kit (Beyotmie
453 Biotechnology, Haimen, China). After added with loading buffer, cell lyses were boiled for 10
454 min at 100˚C for SDS-polyacrylamide gel electrophoresis (PAGE). Proteins were transferred to
455 nitrocellulose (NC) membranes. The membranes were blocked with 5% skim milk at room
456 temperature for 2 h, and then incubated overnight at 4˚C with primary antibodies. After
457 washing the membrane with TBST (TBS, 0.05% Tween-20) /TBS three times (5 min per wash),
458 blots were incubated with the secondary antibody (1:5000) at room temperature for 2 h.
459 Finally, the blots were washed in TBST/TBS. The antibody-reactive bands were revealed by
460 enhanced chemiluminescence (ECL) and exposed on Kodak radiographic film.

461 **Acknowledgment**

462 We are grateful for the financial support from the
463 National Natural Science Foundation of China (No. 81430085 & 21372206); Ph.D Educational
464 Award from Ministry of Education (No. 20134101130001); Outstanding Young Talent Researc
465 h Fund of Zhengzhou University (No. 1521331002); Key Scientific Research Project for Higher
466 Education by Department of Education of Henan Province He'nan Educational Committee (N
467 o. 15A350018); National Natural Science Foundation of Youth Fundation (No. 81602961).

468 **References**

469 [1] Y. Shi, F. Lan, C. Matson, P. Mulligan, J. R. Whetstine, P. A. Cole, R. A. Casero, Y. Shi. Histone
470 Demethylation Mediated by the Nuclear Amine Oxidase Homolog LSD1. *Cell*, 119 (2004)
471 941-953.

472 [2] F. Forneris, C. Binda, M. A. Vanoni, A. Mattevi, E. Battaglioli. Histone demethylation catalysed
473 by LSD1 is a flavin-dependent oxidative process. *FEBS Letters*, 579 (2005) 2203-2207.

474 [3] J. Huang, R. Sengupta, A. B. Espejo, M. G. Lee, J. A. Dorsey, M. Richter, S. Opravil, R. Shiekhattar,
475 M. T. Bedford, T. Jenuwein, S. L. Berger. p53 is regulated by the lysine demethylase LSD1.
476 *Nature*, 449 (2007) 105-108.

477 [4] J. Wang, S. Hevi, J. K. Kurash, H. Lei, F. Gay, J. Bajko, H. Su, W. Sun, H. Chang, G. Xu, F. Gaudet,
478 E. Li, T. Chen. The lysine demethylase LSD1 (KDM1) is required for maintenance of global DNA
479 methylation. *Nat Genet*, 41 (2009) 125-129.

480 [5] S. Amente, L. Lania, B. Majello. The histone LSD1 demethylase in stemness and cancer
481 transcription programs. *Biochimica et Biophysica Acta (BBA) - Gene Regulatory Mechanisms*,
482 1829 (2013) 981-986.

483 [6] Y. Chen , W. Jie, W. Yan, K. Zhou, Y. Xiao. Lysine-specific histone demethylase 1 (LSD1): A
484 potential molecular target for tumor therapy. *Critical Reviews™ in Eukaryotic Gene Expression*,
485 22 (2012) 53-59.

486 [7] K. Sakamoto, T. Imamura, M. Yano, H. Yoshida, A. Fujiki, Y. Hirashima, H. Hosoi. Sensitivity of
487 MLL-rearranged AML cells to all-trans retinoic acid is associated with the level of H3K4me2 in
488 the RAR[alpha] promoter region. *Blood Cancer Journal*, 4 (2014) e205.

489 [8] Z. Feng, Y. Yao, C. Zhou, F. Chen, F. Wu, L. Wei, W. Liu, S. Dong, M. Redell, Q. Mo.
490 Pharmacological inhibition of LSD1 for the treatment of MLL-rearranged leukemia. *Journal of*
491 *hematology & oncology*, 9 (2016) 24-36.

492 [9] S. Hayami, J. D. Kelly, H.-S. Cho, M. Yoshimatsu, M. Unoki, T. Tsunoda, H. I. Field, D. E. Neal, H.
493 Yamaue, B. A. J. Ponder, Y. Nakamura, R. Hamamoto. Overexpression of LSD1 contributes to
494 human carcinogenesis through chromatin regulation in various cancers. *International Journal*
495 *of Cancer*, 128 (2011) 574-586.

496 [10] H. Mohammad, K. Smitheman, M. Cusan, Y. Liu, M. Pappalardi, K. Federowicz, G. Van Aller, J.
497 Kasparec, X. Tian, D. Suarez, M. Rouse, J. Schneck, J. Carson, P. McDevitt, T. Ho, C. McHugh, W.
498 Miller, N. Johnson, S. A. Armstrong, P. Tummino. Inhibition Of LSD1 As a Therapeutic Strategy
499 For The Treatment Of Acute Myeloid Leukemia. *Blood*, 122 (2013) 3964-3964.

500 [11] L. Jin, Christin L. Hanigan, Y. Wu, W. Wang, Ben H. Park, Patrick M. Woster, Robert A. Casero.
501 Loss of LSD1 (lysine-specific demethylase 1) suppresses growth and alters gene expression of
502 human colon cancer cells in a p53- and DNMT1(DNA methyltransferase 1)-independent
503 manner. *Biochemical Journal*, 449 (2013) 459-468.

504 [12] Y. Wu, B. P. Zhou. Epigenetic regulation of LSD1 during mammary carcinogenesis. *Molecular &*
505 *Cellular Oncology*, 1 (2014) e963426.

506 [13] J. H. Schulte, S. Lim, A. Schramm, N. Friedrichs, J. Koster, R. Versteeg, I. Ora, K. Pajtler, L.
507 Klein-Hitpass, S. Kuhfittig-Kulle, E. Metzger, R. Schüle, A. Eggert, R. Buettner, J. Kirfel.
508 Lysine-Specific Demethylase 1 Is Strongly Expressed in Poorly Differentiated Neuroblastoma:
509 Implications for Therapy. *Cancer Research*, 69 (2009) 2065-2071.

[14] J. A. Pollock, M. D. Larrea, J. S. Jasper, D. P. McDonnell, D. G. McCafferty. Lysine-Specific Histone Demethylase 1 Inhibitors Control Breast Cancer Proliferation in ERα-Dependent and -Independent Manners. *ACS Chemical Biology*, 7 (2012) 1221-1231.

[15] Y.-C. Zheng, J. Ma, Z. Wang, J. Li, B. Jiang, W. Zhou, X. Shi, X. Wang, W. Zhao, H.-M. Liu. A Systematic Review of Histone Lysine-Specific Demethylase 1 and Its Inhibitors. *Medicinal Research Reviews*, 35 (2015) 1032-1071.

[16] G. Stazi, C. Zwergel, S. Valente, A. Mai. LSD1 inhibitors: a patent review (2010-2015). *Expert Opinion on Therapeutic Patents*, 26 (2016) 565-580.

[17] Lee, Choi, Doh, Jung, Chai. Effects of the monoamine oxidase inhibitors pargyline and tranylcypromine on cellular proliferation in human prostate cancer cells. *Oncology Reports*, 30 (2013) 1587-1592.

[18] S. Mimasu, N. Umezawa, S. Sato, T. Higuchi, T. Umehara, S. Yokoyama. Structurally Designed trans-2-Phenylcyclopropylamine Derivatives Potently Inhibit Histone Demethylase LSD1/KDM1. *Biochemistry*, 49 (2010) 6494-6503.

[19] Y.-C. Zheng, B. Yu, Z.-S. Chen, Y. Liu, H.-M. Liu. TCPs: privileged scaffolds for identifying potent LSD1 inhibitors for cancer therapy. *Epigenomics*, 8 (2016) 651-666.

[20] Y. C. Zheng, B. Yu, G. Z. Jiang, X. J. Feng, P. X. He, X. Y. Chu, W. Zhao, H. M. Liu. Irreversible LSD1 Inhibitors: Application of Tranylcypromine and Its Derivatives in Cancer Treatment. *Current Topics in Medicinal Chemistry*, 16 (2016) 2179-2188.

[21] Helai P. Mohammad, Kimberly N. Smitheman, Chandrashekhar D. Kamat, D. Soong, Kelly E. Federowicz, Glenn S. Van Aller, Jess L. Schneck, Jeffrey D. Carson, Y. Liu, M. Butticello, William G. Bonnette, Shelby A. Gorman, Y. Degenhardt, Y. Bai, Michael T. McCabe, Melissa B. Pappalardi, J. Kasparec, X. Tian, Kenneth C. McNulty, M. Rouse, P. McDevitt, T. Ho, M. Crouthamel, Timothy K. Hart, Nestor O. Concha, Charles F. McHugh, William H. Miller, D. Dhanak, Peter J. Tummino, Christopher L. Carpenter, Neil W. Johnson, Christine L. Hann, Ryan G. Kruger. A DNA Hypomethylation Signature Predicts Antitumor Activity of LSD1 Inhibitors in SCLC. *Cancer Cell*, 28 (2015) 57-69.

[22] P. Gallipoli, G. Giotopoulos, B. J. P. Huntly. Epigenetic regulators as promising therapeutic targets in acute myeloid leukemia. *Therapeutic Advances in Hematology*, 6 (2015) 103-119.

[23] L.-Y. Ma, Y.-C. Zheng, S.-Q. Wang, B. Wang, Z.-R. Wang, L.-P. Pang, M. Zhang, J.-W. Wang, L. Ding, J. Li, C. Wang, B. Hu, Y. Liu, X.-D. Zhang, J.-J. Wang, Z.-J. Wang, W. Zhao, H.-M. Liu. Design, Synthesis, and Structure–Activity Relationship of Novel LSD1 Inhibitors Based on Pyrimidine–Thiourea Hybrids As Potent, Orally Active Antitumor Agents. *Journal of Medicinal Chemistry*, 58 (2015) 1705-1716.

[24] Y.-C. Zheng, Y.-C. Duan, J.-L. Ma, R.-M. Xu, X. Zi, W.-L. Lv, M.-M. Wang, X.-W. Ye, S. Zhu, D. Mobley, Y.-Y. Zhu, J.-W. Wang, J.-F. Li, Z.-R. Wang, W. Zhao, H.-M. Liu. Triazole–Dithiocarbamate Based Selective Lysine Specific Demethylase 1 (LSD1) Inactivators Inhibit Gastric Cancer Cell Growth, Invasion, and Migration. *Journal of Medicinal Chemistry*, 56 (2013) 8543-8560.

549 [25] X.-W. Ye, Y.-C. Zheng, Y.-C. Duan, M.-M. Wang, B. Yu, J.-L. Ren, J.-L. Ma, E. Zhang, H.-M. Liu.
550 Synthesis and biological evaluation of coumarin-1,2,3-triazole-dithiocarbamate hybrids as
551 potent LSD1 inhibitors. *MedChemComm*, 5 (2014) 650-654.

552 [26] B. Yu, P.-P. Qi, X.-J. Shi, R. Huang, H. Guo, Y.-C. Zheng, D.-Q. Yu, H.-M. Liu. Efficient synthesis of
553 new antiproliferative steroidal hybrids using the molecular hybridization approach. *European*
554 *Journal of Medicinal Chemistry*, 117 (2016) 241-255.

555 [27] D. P. Mould, A. E. McGonagle, D. H. Wiseman, E. L. Williams, A. M. Jordan. Reversible Inhibitors
556 of LSD1 as Therapeutic Agents in Acute Myeloid Leukemia: Clinical Significance and Progress to
557 Date. *Medicinal Research Reviews*, 35 (2015) 586-618.

558 [28] M. E. Matyskiela, G. Lu, T. Ito, B. Pagarigan, C.-C. Lu, K. Miller, W. Fang, N.-Y. Wang, D. Nguyen,
559 J. Houston, G. Carmel, T. Tran, M. Riley, L. A. Nosaka, G. C. Lander, S. Gaidarova, S. Xu, A. L.
560 Ruchelman, H. Handa, J. Carmichael, T. O. Daniel, B. E. Cathers, A. Lopez-Girona, P. P.
561 Chamberlain. A novel cereblon modulator recruits GSPT1 to the CRL4CRBN ubiquitin ligase.
562 *Nature*, 535 (2016) 252-257.

563 [29] J. Krönke, N. D. Udeshi, A. Narla, P. Grauman, S. N. Hurst, M. McConkey, T. Svinkina, D. Heckl, E.
564 Comer, X. Li, C. Ciarlo, E. Hartman, N. Munshi, M. Schenone, S. L. Schreiber, S. A. Carr, B. L.
565 Ebert. Lenalidomide Causes Selective Degradation of IKZF1 and IKZF3 in Multiple Myeloma
566 Cells. *Science*, 343 (2014) 301-305.

567 [30] G. Lu, R. E. Middleton, H. Sun, M. Naniong, C. J. Ott, C. S. Mitsiades, K.-K. Wong, J. E. Bradner,
568 W. G. Kaelin. The Myeloma Drug Lenalidomide Promotes the Cereblon-Dependent Destruction
569 of Ikaros Proteins. *Science*, 343 (2014) 305-309.

570 [31] G. E. Winter, D. L. Buckley, J. Paulk, J. M. Roberts, A. Souza, S. Dhe-Paganon, J. E. Bradner.
571 Phthalimide conjugation as a strategy for in vivo target protein degradation. *Science*, 348 (2015)
572 1376-1381.

573 [32] B. Yu, X.-J. Shi, Y.-F. Zheng, Y. Fang, E. Zhang, D.-Q. Yu, H.-M. Liu. A novel [1,2,4] triazolo [1,5-a]
574 pyrimidine-based phenyl-linked steroid dimer: Synthesis and its cytotoxic activity. *European*
575 *Journal of Medicinal Chemistry*, 69 (2013) 323-330.

576 [33] L.-H. Huang, Y.-F. Zheng, Y.-Z. Lu, C.-J. Song, Y.-G. Wang, B. Yu, H.-M. Liu. Synthesis and
577 biological evaluation of novel steroidal[17,16-d][1,2,4]triazolo[1,5-a]pyrimidines. *Steroids*, 77
578 (2012) 710-715.

579 [34] G. Shao, J. Wang, Y. Li, X. Liu, X. Xie, X. Wan, M. Yan, J. Jin, Q. Lin, H. Zhu, L. Zhang, A. Gong, Q.
580 Shao, C. Wu. Lysine-specific demethylase 1 mediates epidermal growth factor signaling to
581 promote cell migration in ovarian cancer cells. *Scientific Reports*, 5 (2015) 15344.

582 [35] T. Lv, D. Yuan, X. Miao, Y. Lv, P. Zhan, X. Shen, Y. Song. Over-Expression of LSD1 Promotes
583 Proliferation, Migration and Invasion in Non-Small Cell Lung Cancer. *PLoS ONE*, 7 (2012)
584 e35065.

Highlights

- A new series of [1,2,4]triazolo[1,5-a]pyrimidine-based analogs were designed and synthesized
- Compound **5p** inactivated LSD1 potently (IC_{50} = 154 nM)
- Docking studies were performed to rationalize the potency against LSD1
- Compound **5p** inhibited migration of MGC-803 and PC-9 cells
- Compound **6l** showed excellent growth inhibition toward MGC-803 and PC-9 cells